Transportation Research Part C 60 (2015) 324–338

Contents lists available at ScienceDirect

Transportation Research Part C

journal homepage: www.elsevier.com/locate/trc

Understanding the structure of hyper-congested traffic from empirical and experimental evidences

Cheng-Jie Jin [a,b], Wei Wang [a,b], Rui Jiang [c,d,*], H.M. Zhang [e,f], Hao Wang [a,b], Mao-Bin Hu [d]

[a] Jiangsu Key Laboratory of Urban ITS, Southeast University of China, Nanjing, Jiangsu 210096, People's Republic of China
[b] Jiangsu Province Collaborative Innovation Center of Modern Urban Traffic Technologies, Nanjing, Jiangsu 210096, People's Republic of China
[c] MOE Key Laboratory for Urban Transportation Complex Systems Theory and Technology, Beijing Jiaotong University, Beijing 100044, People's Republic of China
[d] School of Engineering Science, University of Science and Technology of China, Hefei, Anhui 230026, People's Republic of China
[e] Department of Traffic Engineering, School of Transportation Engineering, Tongji University, Shanghai 200092, People's Republic of China
[f] Department of Civil and Env. Engineering, University of California, Davis, USA

ARTICLE INFO

Article history:
Received 11 February 2015
Received in revised form 15 July 2015
Accepted 16 September 2015

Keywords:
Traffic flow
Homogeneous congested traffic
Hyper congestion

ABSTRACT

We study in this paper the structure of traffic under hypercongestion, which is a controversial issue between traditional two-phase traffic theory and Kerner's three-phase theory. By analyzing video traffic data from a section of the Nanjing Airport Highway, it is found that traffic states inside hypercongestion are not homogeneous, which contradicts the existence of a "Homogeneous Congested Traffic" state claimed in two-phase traffic theory. Analysis of vehicle trajectories and velocities obtained from an experimental car-following study with a platoon of 25 vehicles also confirms the above findings. Furthermore, it is also found from the video traffic data that the structure of hypercongested traffic varies only slightly with location, which might be due to small jams inside hypercongested traffic merging into larger ones slowly and/or larger jams sometimes breaking into small ones. Finally, the implications of our observations on traffic modeling have been discussed.

1. Introduction

The structure of traffic flow, namely the time-space patterns of various traffic state variables (such as flow, headway, speed and spacing) and their manifestations in the corresponding phase space (such as speed-spacing, flow-density phase space) provides a critical understanding of traffic dynamics and essential models for traffic control.

To understand the structure of traffic flow, many empirical studies have been performed. These empirical studies usually use the time series of flow rate and average occupancies or velocities obtained at different loop detectors to construct spatiotemporal diagrams of traffic flow (e.g., Kerner and Rehborn, 1997; Kerner, 1998; Schönhof and Helbing, 2007, 2009; Treiber et al., 2010; Treiber and Kesting, 2012) or use the event data that record the times when a vehicle arrives at and departs from a loop detector (Wu and Liu, 2014). The curves of cumulative vehicle count and the curves of cumulative occupancy are also used for the visual identification of time-dependent features of traffic streams see, e.g., Windover and Cassidy (2001). Moreover, the NGSIM data, which provide vehicle trajectories, have been used to analyze evolution of traffic oscillations, see e.g., Li et al. (2012). On the other hand, many traffic flow models have been proposed to simulate traffic flow. For

* Corresponding author at: MOE Key Laboratory for Urban Transportation Complex Systems Theory and Technology, Beijing Jiaotong University, Beijing 100044, People's Republic of China.
E-mail addresses: rjiang@ustc.edu.cn (R. Jiang), hmzhang@ucdavis.edu (H.M. Zhang).

http://dx.doi.org/10.1016/j.trc.2015.09.007
0968-090X/

some recent models, see e.g., Saifuzzaman and Zheng (2014), Tian et al. (2014, 2015), Kim et al. (2013), Schnetzler and Louis (2013), Farhi (2012), Laval et al. (2014), and Li et al. (2013).

Despite the vast amount of empirical data and numerous models, both the spatiotemporal and phase structures of traffic flow are still not well understood, leading to a few controversies in traffic flow studies, see e.g., Daganzo et al. (1999), Schönhof and Helbing (2007, 2009), Treiber et al. (2010) and Kerner (2013). This paper focuses on one particular controversial issue, i.e., the structure of hypercongested traffic. In this paper, hypercongestion is defined as a seriously congested traffic state with flow rate below 700 vehicles/h/lane (about 1/3 of regular capacity). Hypercongestion on highways and city expressways is usually induced by, for example, serious accidents with lane closures and bad weather.[1]

In traffic modeling, it is usually assumed that there exists a fundamental diagram (FD), which describes the unique relationship between flow rate and traffic density in the steady state (Helbing, 2001). Traditionally the fundamental diagram is assumed to be concave. To our knowledge, Kerner and Konhäuser (1993) are among the first to study the implications of the fundamental diagram with a turning point (concave–convex FDs) on traffic flow. As a result, traffic density could be classified into stable, unstable and metastable range as shown in Fig. 1. Helbing et al. (1999) studied the traffic flow features induced by an isolated bottleneck. It is shown that when a hypercongestion state is induced by a strong bottleneck, so that the traffic density exceeds the critical density ρ_{c4} in the diagram, traffic flow will be stable. Vehicles in the traffic move with homogeneous and slow (but not necessarily zero) speed, and the state is named as homogeneous congested traffic (HCT). When the bottleneck strength decreases and traffic density is below ρ_{c4}, the traffic will lose stability and exhibit oscillating behavior and thus is named as oscillating congested traffic (OCT).[2] Helbing et al. have reported HCT observed in real traffic, which requires large bottleneck strengths (with flows below 700 vehicles per hour per lane) (Schönhof and Helbing, 2007).

Nevertheless, Kerner (2008) pointed out that the empirical evidence of the HCT is invalid, due to the way the average speeds are computed. In the raw data used by Schönhof and Helbing (2007), if the speeds (v) of all vehicles that have passed a detector during a 1 min interval are within the range $0 < v < 20$ km/h, then the average speed is set to 10 km/h by the road computer. Only if no vehicle passes a detector during a 1 min interval, the computer sets the average speed to zero. Thus, in the low speed data, there are mostly two speed values, zero and 10 km/h. Moreover, the adaptive smoothing method has been used to process the raw data. As a result, the speed cannot be used to decide whether the speed distribution is a homogeneous one or not.

In Kerner's empirical example (Kerner, 2008), the arithmetical averaging of single-vehicle speeds of vehicles passing a detector during each 1 min interval is used. In measured data associated with bad weather conditions, the flow rate is 513 vehicles/h/lane on average, and an inhomogeneous spatiotemporal structure of congestion is observed. To explain this and other features of traffic flow, Kerner (2004, 2009) has proposed a three-phase traffic theory. The main idea is that there is no fundamental diagram in traffic flow. Instead, the steady state of traffic flow occupies a 2D region in the flow density plane, in which drivers do not care about the spacing for a given speed, as long as the spacing is within the range given by this 2D region.

In both cases, the data used are from the traditional loop detectors, and are 1-min-averaged velocities or flow rates. It is possible that the different conclusions drawn in these studies are due to the limitation of the low resolution data. Therefore, the data are not adequate, in some researchers' viewpoint, to draw an unambiguous conclusion. For example, in their paper published two years later than Kerner's paper, Treiber et al. (2010) claimed "*For strong bottlenecks (typically caused by accidents), empirical evidence regarding the existence of homogeneous congested traffic has been somewhat ambiguous so far*". Kerner (2008) also claimed that to study the structure of hypercongestion, "*single-vehicle data measured within traffic congestion at heavy bottlenecks is required*" *and it is* "*a separate and important task of further investigation*".

In this study, we use high resolution, individual vehicle data from both videos and car-following experiments to study the structure of traffic flow in hypercongested states. We have collected video data from cameras along the Nanjing Airport Highway on which some heavy congestion due to stopped vehicles has been observed. We have obtained single-vehicle data from the videos by a software named Autoscope Rackvision Terra. It is found that inside hypercongestion, the traffic data (including single-vehicle velocities and time-headways, and 30-s-averaged flow rate) are not homogeneous over 30 min on the 3000 m long road segment, having no HCT states. We have carried out an experimental study of car-following behavior in a platoon with 25 vehicles and extracted vehicle trajectories and velocities. HCT states are not found in the experimental data as well.

The rest of this paper is organized as follows. The analysis of empirical data is discussed in Section 2. In Section 3, the experimental results are presented. Section 4 discusses the implications of our observations on traffic modeling. The conclusion is given in Section 5.

2. Empirical data analysis

The traffic flow data of the Nanjing Airport Highway, which is the main road connecting the urban district with Nanjing Lukou Airport, will be studied in this paper (see Fig. 2). There are 40 cameras along the 28 km-long highway, and in each

[1] Note that Kerner (2008) has used "mega-jam" instead of the term "hypercongestion" used in this paper.

[2] In our previous paper (Jiang et al., 2014), it has been shown that in the formation of OCT, the oscillation initially grows in a convex way. This is not consistent with the experimental findings, in which the oscillation grows in a concave way or linearly, see also Appendix A. This implies that the formation mechanism of OCT (i.e., the linear instability of the steady solution) in Helbing et al. (1999) is not likely to be correct.

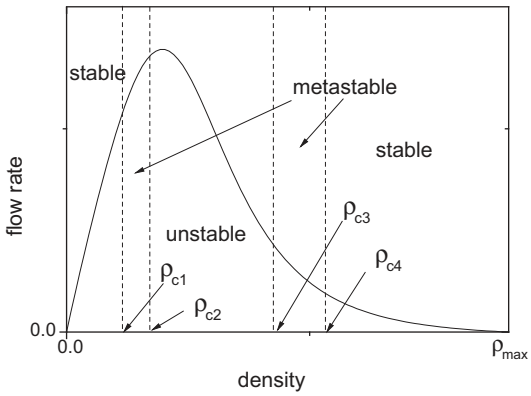

Fig. 1. Sketch of the stable, unstable and metastable density ranges.

direction there are two lanes. The speed limit is 120 km/h. In this paper, all the traffic data presented are taken in the direction from the urban district to the airport.

Our example is a hypercongestion resulted from stopped vehicles about 150 m downstream of Camera 07 on June 15, 2010. Between 9:06 and 10:25, there are two stopped vehicles, one is a large truck, and the other is a small car. The truck occupied the emergency lane and the right part of the right lane. The car only occupied the emergency lane. So there are only 1.5 lanes left for passing. At about 10:25, the truck moved away and two lanes can be used for passing. As a result, the bottleneck strength weakens. At about 11:01, the car also moved away and the congestion disappears from then on. This paper concentrates on the traffic flow before 10:25 induced by the strong bottleneck caused by the truck.

During the time period of congestion, the long queue continuously grows upstream to the location of Camera 03. Camera 03/06/07 is about 3000 m/900 m/150 m upstream of the bottleneck. However, since the cameras may switch for 360° for the convenience of management and they have been switched during the period, the videos are not suitable for image processing between 9:51 and 9:53 at Camera 03, after 9:49 at Camera 06, and after 9:47 at Camera 07. For Camera 07/06/03, the congestion started at about 9:06, 9:16, 9:53, respectively.

The single-vehicle traffic data (single-vehicle velocities and time-headways, and 30-s-averaged flow rate) are extracted by a software named Autoscope Rackvision Terra. To remove some obvious errors, we performed error correction on the data through checking the videos frame by frame by using a software named Tracker. A careful calibration indicates that the estimation errors of speed are within ±1 m/s. We only present data collected on the left lane, since the data on the right lane and on the emergency lane are difficult to measure at Camera 06/07: the vehicles are frequently blocked by large vehicles on the left lane. We would like to mention that when the highway is seriously congested, many drivers have used the emergency lane.

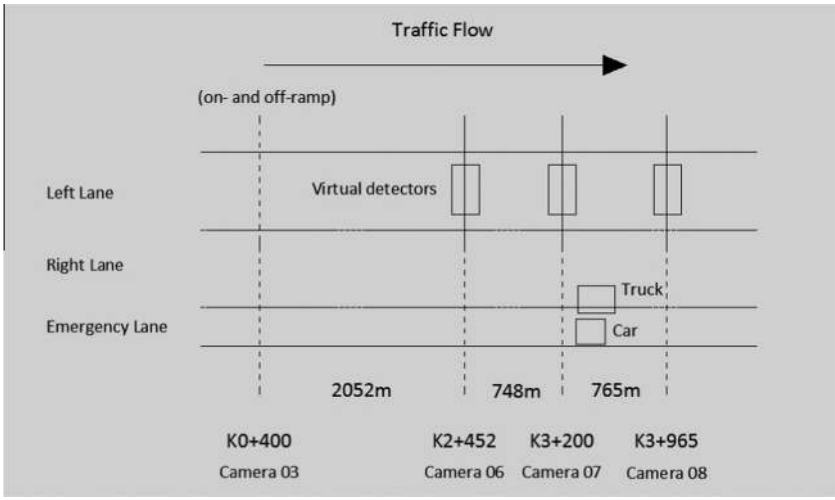

Fig. 2. The sketch of a section of the Nanjing Airport Highway and locations of the cameras. Here K*X* + *Y* is widely used in transportation engineering in China and it means that the camera is 1000*X* + *Y* m away from the highway end. At camera 03, there is an off-ramp. In the vicinity downstream of camera 03, there is an on-ramp.

Due to the existence of the on-ramp and the off-ramp in the vicinity of camera 03, the flow rate on the left lane at camera 03 (about 460 vehicles/h) is smaller than that at cameras 06 and 07 (about 600 vehicles/h).

Fig. 3(a)–(c) shows the vehicle velocities at the three locations, which are obviously inhomogeneous. The stop-and-go phenomena can be clearly observed in the videos at the three locations. Since Autoscope cannot detect the zero velocity when the car stops, only the starting velocity which is a little larger than zero can be recorded and shown in the figures. Fig. 3(d) shows the velocity distribution at the three locations, which are similar to each other.

Fig. 4(a)–(c) shows the vehicle time headways at the three locations, which are also obviously inhomogeneous. There are many large time headways appearing from time to time, which correspond to that of stopped vehicles. When it is far from the bottleneck, as shown in Fig. 4(a), the appearance frequency of large time headways notably decreases. For example, the number of time headways which are larger than 6 s at Camera 03/06/07 are: 75 during 42 min, 80 during 32 min and 97 during 40 min. This, we argue, is because some small jams inside the hyper congested traffic have merged into larger ones. However, at different locations, there is no notable difference among the distributions of velocity (Fig. 3(d)) and the time headway (Fig. 4(d)). This might be due to that the merging of small jams is slow and/or larger jams sometimes break into small ones.

Finally, Fig. 5(a)–(c) shows the 30-s-averaged flow rate at the three locations. One can see that the flow rate varies significantly. Sometimes it is zero (Fig. 5(a)), and sometimes it can even reach 1200 vehicles/h, comparable to that in free flow.

3. Experimental car-following study

We have carried out an experimental car-following study with a platoon of 25 vehicles on 19 January 2013 on a 3.2 km stretch of Chuangxin Avenue in a suburban area in Hefei City, China. Since the road is in a suburban area, there is almost no interference from other vehicles that are not part of the experiment. We have installed a high-precision GPS device on each car to record the location and velocity of the car every 0.1 s. In one of the cars (the 23rd car), we have installed two GPS devices to check the measurement errors of the GPS devices. As shown in Appendix B, the errors are small, which could be ignored in this study.

We have carried out many runs of the experiment, in which the leading car is asked to move with different velocity. For more details of the experiment, one can refer to Jiang et al. (2014). To study the feature of hypercongestion, in two runs of the experiment, the leading car is instructed to move at a constant speed of about 6.8 km/h (the driver is asked not to step on the gas pedal) to form a strong moving bottleneck that induces hypercongested traffic, see the velocity of the 1st car in Figs. 6(a) and 7(a). The average flow rate is about 631 veh/h, which is comparable with the empirical data.

Figs. 6(a) and 7(a) show the velocities of the cars. Figs. 6(b) and 7(b) show trajectories of the cars. One can see that the cars cannot move at constant speeds and spacing (a homogenous state). Rather, small jams are frequently observed at the rear part of the platoon. Our experiment again does not find any HCT state in hypercongested traffic.

To understand the reason why traffic flow cannot remain homogeneous in hypercongestion, we show in Fig. 8 several typical examples of the spacing and velocity of the following car as well as the velocity of the preceding car.

Panels (a) and (b) show that the following car mainly responds to the speed difference and does not respond to the change of spacing, and the spacing fluctuates in a wide range. Panels (c) and (d) show another two examples, in which the following car is in a no-response state that does not respond to either the small speed difference or the change of spacing. When the spacing has become large enough, the following car accelerates to narrow the spacing. Then the following car goes into the no-response state again.

Panels (e) and (f) show example of the 15th car in two different runs of the experiment, in which the 15th car keeps a small spacing from the 14th car. Since it is dangerous, after some time, the driver brakes (indicated by black arrows) to avoid potential collision.

To summarize, when the velocity difference is not large, the spacing changes but the driver usually does not care and does not respond to the change unless the spacing becomes too large or too small. When the spacing becomes too large or too small, the driver will accelerate to narrow the spacing or decelerate to avoid potential collision. This acceleration or deceleration disturbs the traffic flow. With the propagation and evolution of such disturbances, traffic flow becomes unstable.

4. Discussion

We would like to point out that some large gaps can be observed as indicated by the arrows in Figs. 6(b) and 7(b). This is because sometimes some drivers would not follow closely to the preceding car. Otherwise, he/she has to brake and accelerate incessantly. Since no car will cut in, these drivers prefer to drive in a relaxed way. This driving behavior has also been observed on single-lane highway (Jin et al., 2014). One can imagine that this driving behavior will be strongly suppressed in multilane roads, because cars on other lanes can cut in if a driver leaves a large gap.

There have been quite a few efforts of developing car-following models to reproduce traffic oscillations observed in the NGSIM data, see e.g., Ahn et al. (2013), Chen et al. (2012a, 2012b, 2014), Laval and Leclercq (2010), Laval et al. (2014), Jabari and Liu (2012), Jabari et al. (2014) and Zheng et al. (2011a, 2011b). These models have not been examined against hypercongestion conditions and it is still unclear if they can reproduce the inhomogeneous structure of hypercongestion observed

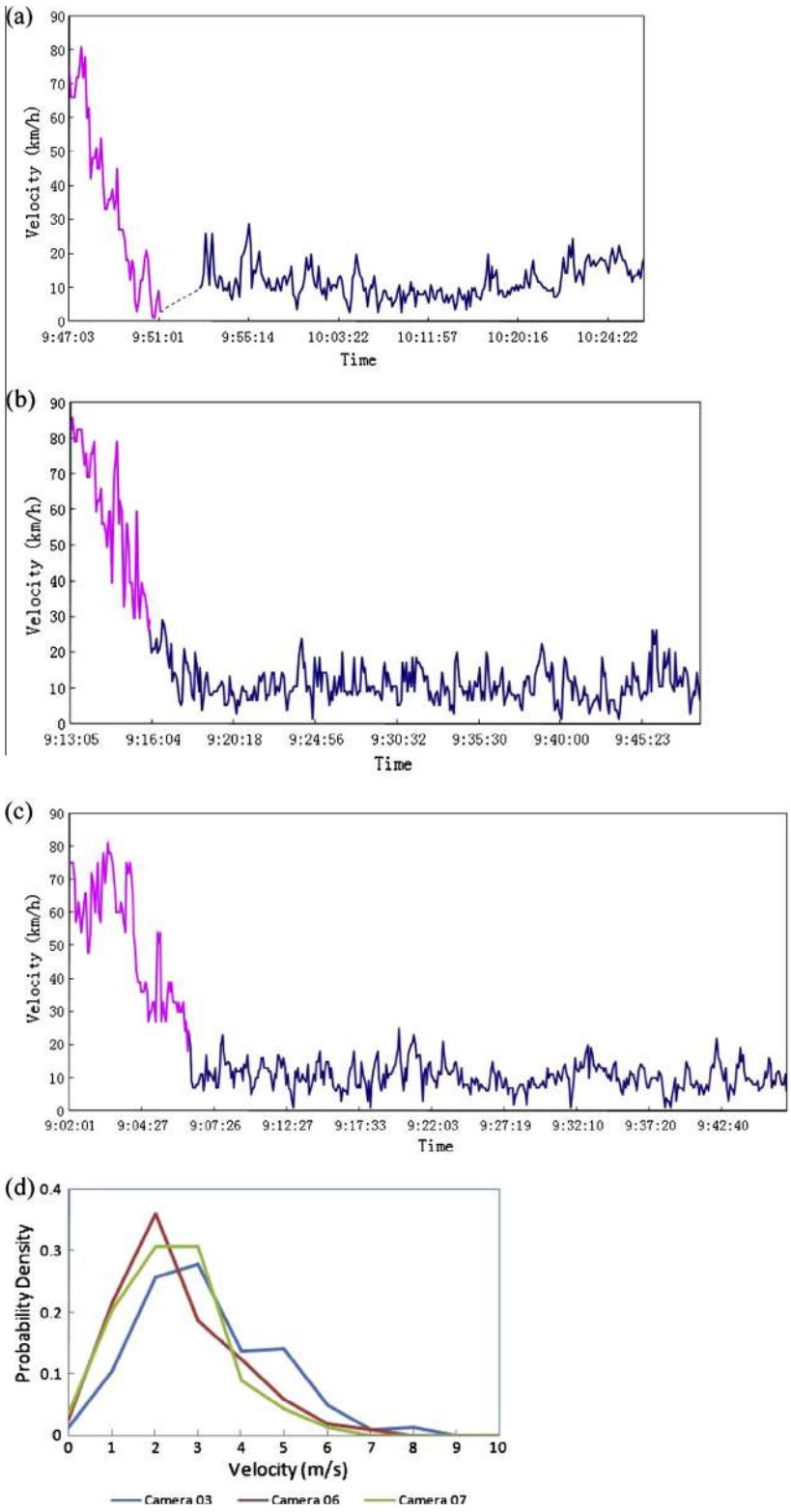

Fig. 3. The time series of vehicle velocities, collected on June 15, 2010 by (a) Camera 03, (b) Camera 06 and (c) Camera 07. Magenta curves show the vehicle velocities several minutes before the hyper congested traffic propagates to the camera locations. Blue curves correspond to the vehicle velocities inside the hypercongested traffic. In (a), the dotted line represents the short time span (2 min) which are not available. (d) shows the velocity distribution in the hypercongested traffic at the three camera locations. Here all the data are collected on the left lane. (For interpretation of the references to color in this figure legend, the reader is referred to the web version of this article.)

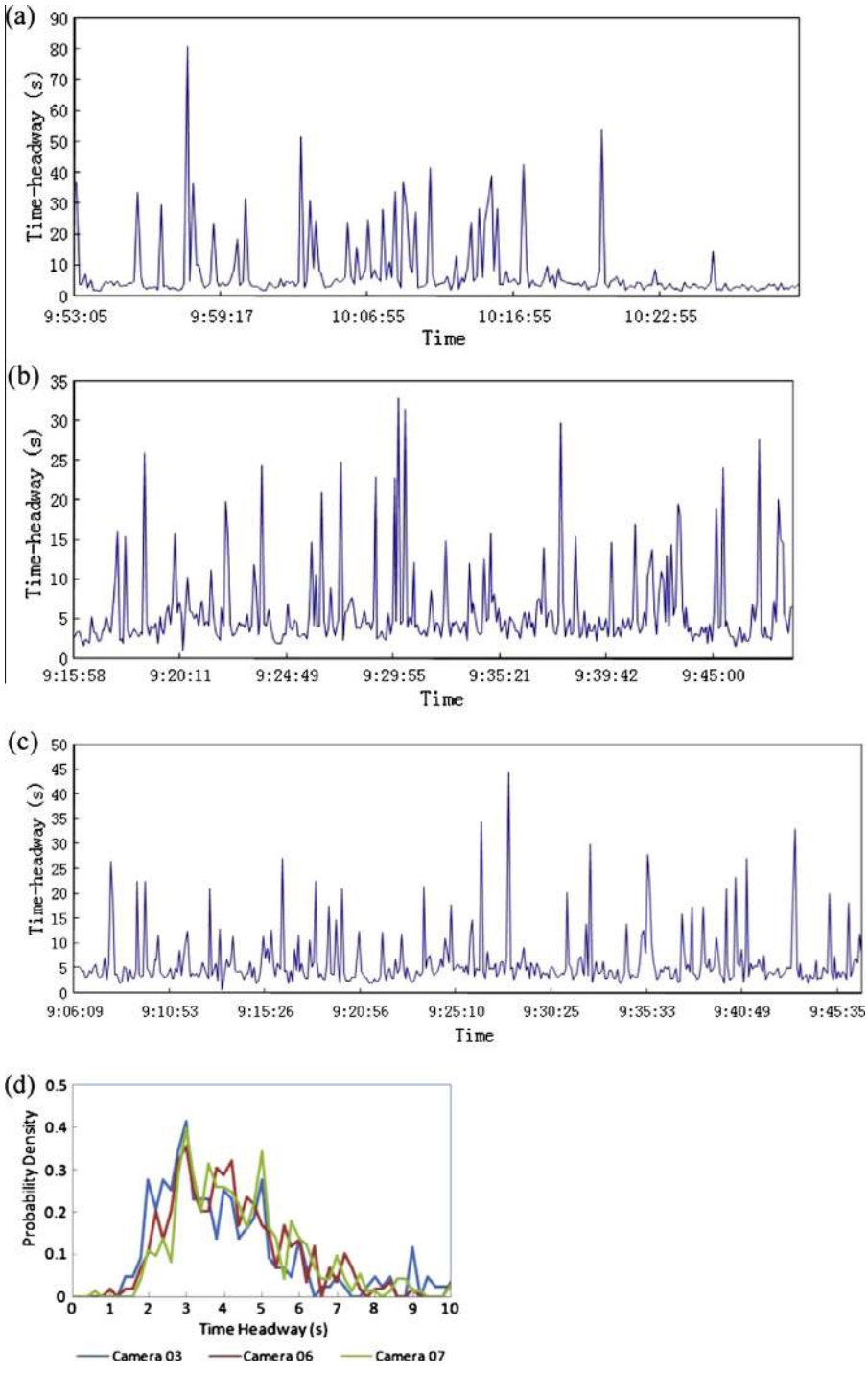

Fig. 4. (a–c) The time series of vehicle time-headways inside the hypercongested traffic (corresponding to the blue curves of Fig. 3). (d) shows the time-headway distribution in the hypercongested traffic at the three camera locations. Here all the data are collected on the left lane.

in our field data and car-following experiments. Note that the oscillations observed in the NGSIM data are very different from the inhomogeneous structure of hypercongestion. For example, in the US101 data, the average flow rate is about 1600–1800 vehicles/h/lane, which is remarkably larger than that in hypercongestion (below 700 vehicles/h/lane).

Next we discuss the implications of our observations on traffic modeling, in terms of several typical traffic flow models.

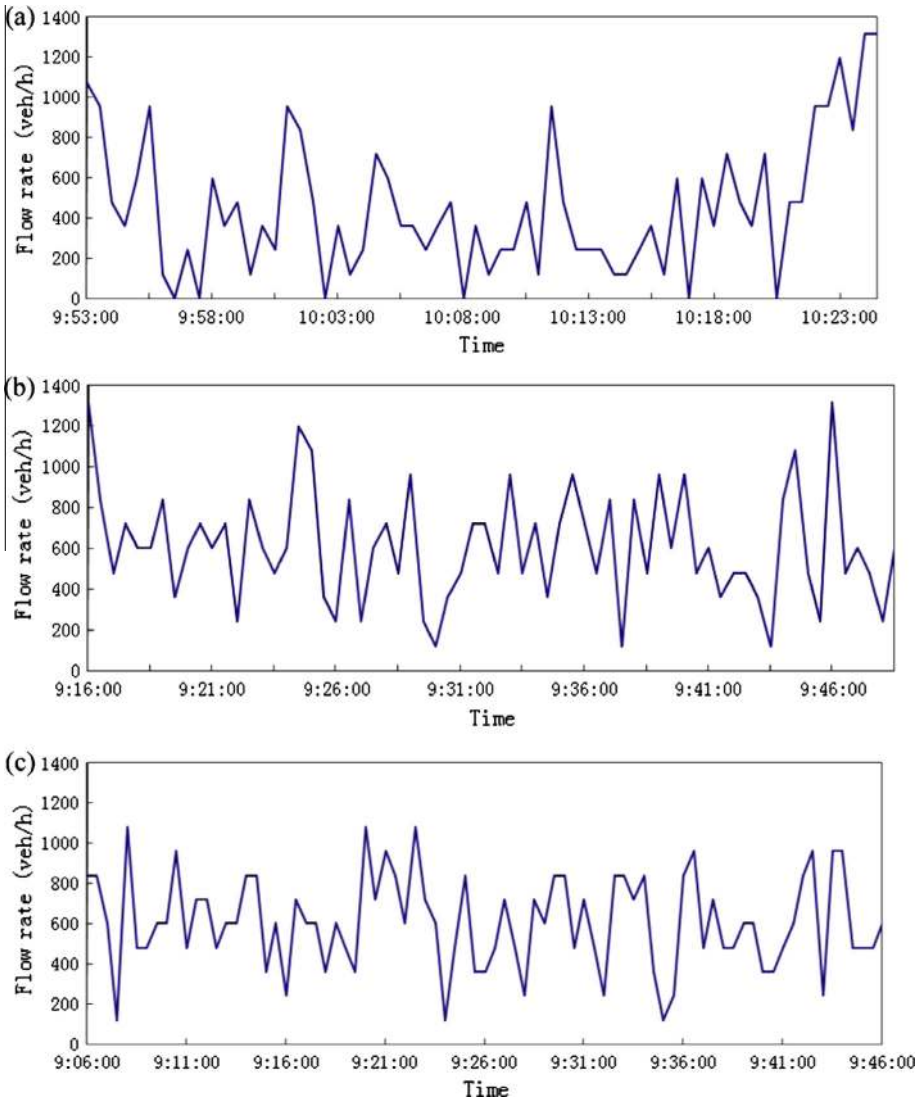

Fig. 5. The time series of 30-s-averaged flow rate inside the hypercongested traffic (corresponding to the blue curves of Fig. 3).

4.1. Intelligent driver model

Our earlier work (Jiang et al., 2014) demonstrated that the commonly used car-following models cannot reproduce the inhomogeneous states observed in the experiments and field data. Yet Treiber et al. (2010) claimed that many models with a fundamental diagram can be calibrated in a way that generates either homogeneous or inhomogeneous patterns of hypercongested traffic. In particular, they have proposed a set of parameters for the intelligent driver model (IDM) and showed that the hypercongested flow is inhomogeneous.

To compare Treiber et al. (2010)'s results with our experimental findings, we now carry out simulations using the IDM model and the parameters proposed in Treiber et al. (2010). In our simulations, we use the vehicle trajectory of the leading car in our experiments as the boundary input. The IDM reads (Treiber et al., 2000)

$$\frac{dv_i}{dt} = a\left[1 - \left(\frac{v_i}{v_{\max}}\right)^4 - \left(\frac{s_0 + v_i T + \frac{v_i(v_i - v_{i-1})}{2\sqrt{ab}}}{x_{i-1} - x_i - l}\right)^2\right]$$

and the parameters are $v_{\max} = 120$ km/h, $T = 1$ s, $s_0 = 2$ m, $a = 1.2$ m/s^2, and $b = 1.3$ m/s^2. Here x_i and v_i denote location and velocity of car i, and car i follows car $i-1$, a is maximum acceleration, b is desired deceleration, T is desired time headway, s_0 is the desired gap (bumper-to-bumper distance) between two neighboring cars in jam, $v_{\max}$ is maximum velocity, l is car length and is set as 5 m.

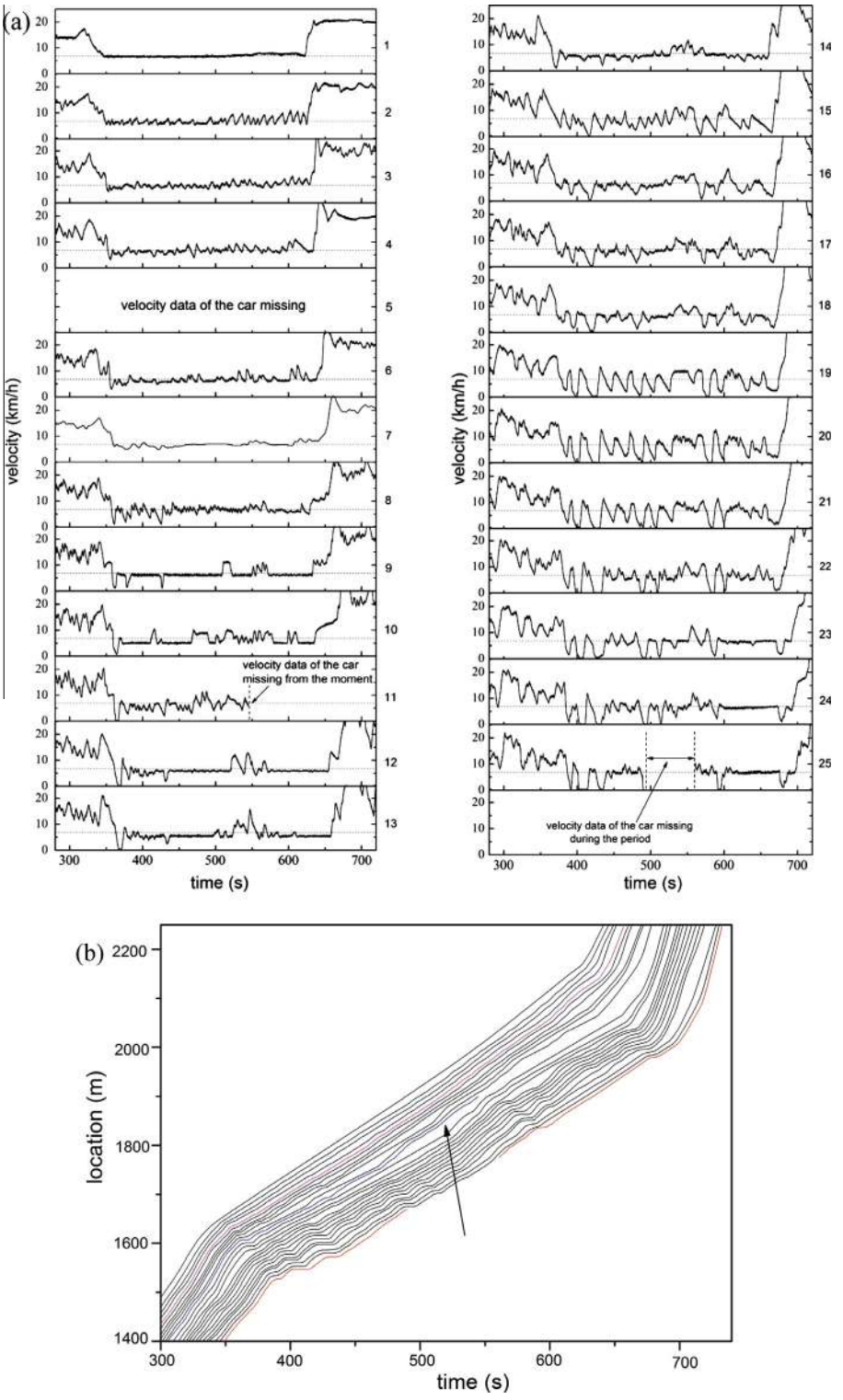

Fig. 6. (a) Velocity of the cars in one run of the experiment. The dashed line shows velocity 6.8 km/h. (b) Trajectories of the cars. Note that the GPS on the 11th car and the 25th car sometimes fail to record the velocity and the location information due to temporary loss of signal. The GPS on the 5th car records only location information (the Magenta line) due to device problem. (For interpretation of the references to color in this figure legend, the reader is referred to the web version of this article.)

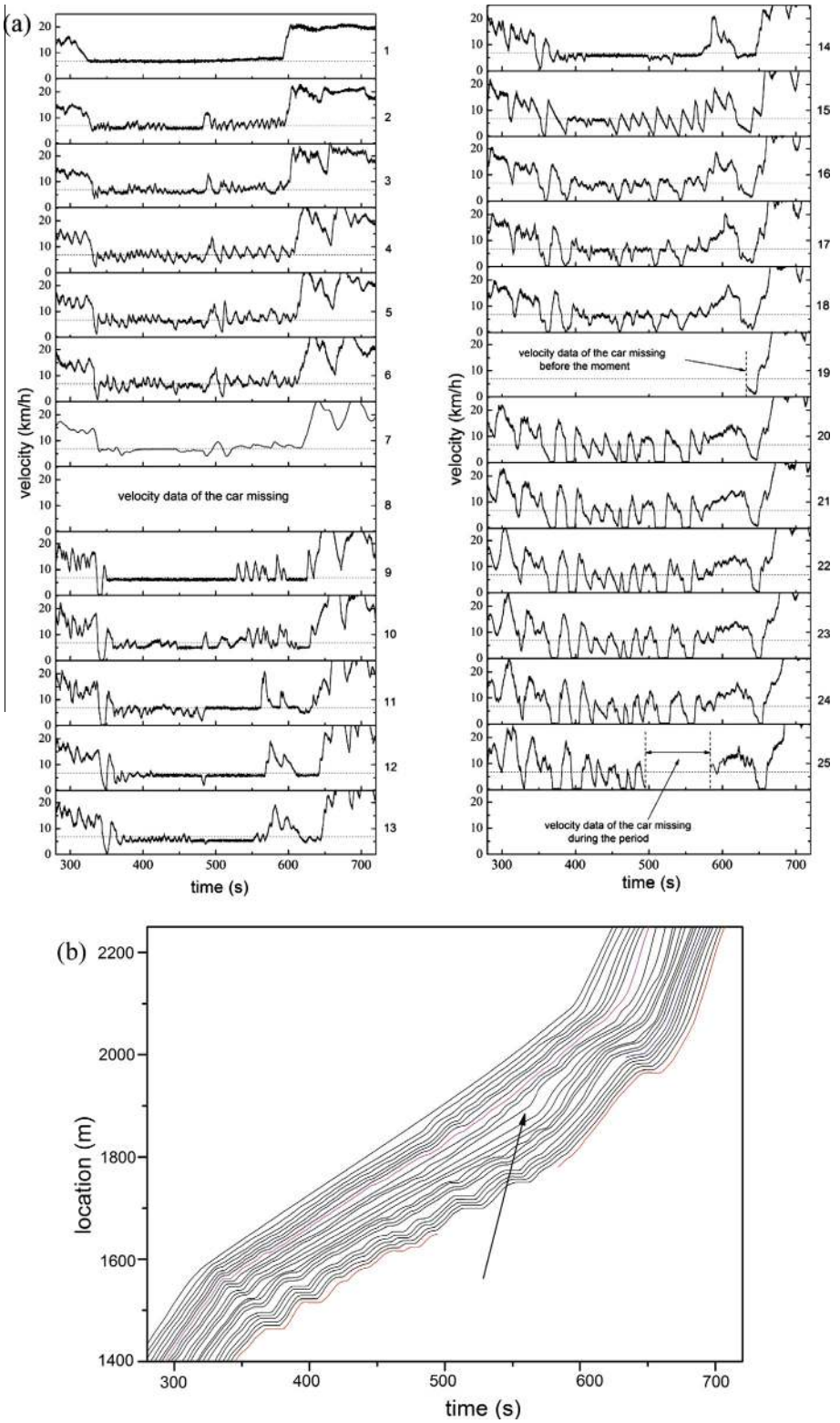

Fig. 7. (a) Velocity of the cars in another run of the experiment. The dashed line shows velocity 6.8 km/h. (b) Trajectories of the cars. Note that the GPS on the 19th car and the 25th car sometimes fail to record the velocity and the location information due to temporary loss of signal. The GPS on the 8th car records only location information (the Magenta line) due to device problem. (For interpretation of the references to color in this figure legend, the reader is referred to the web version of this article.)

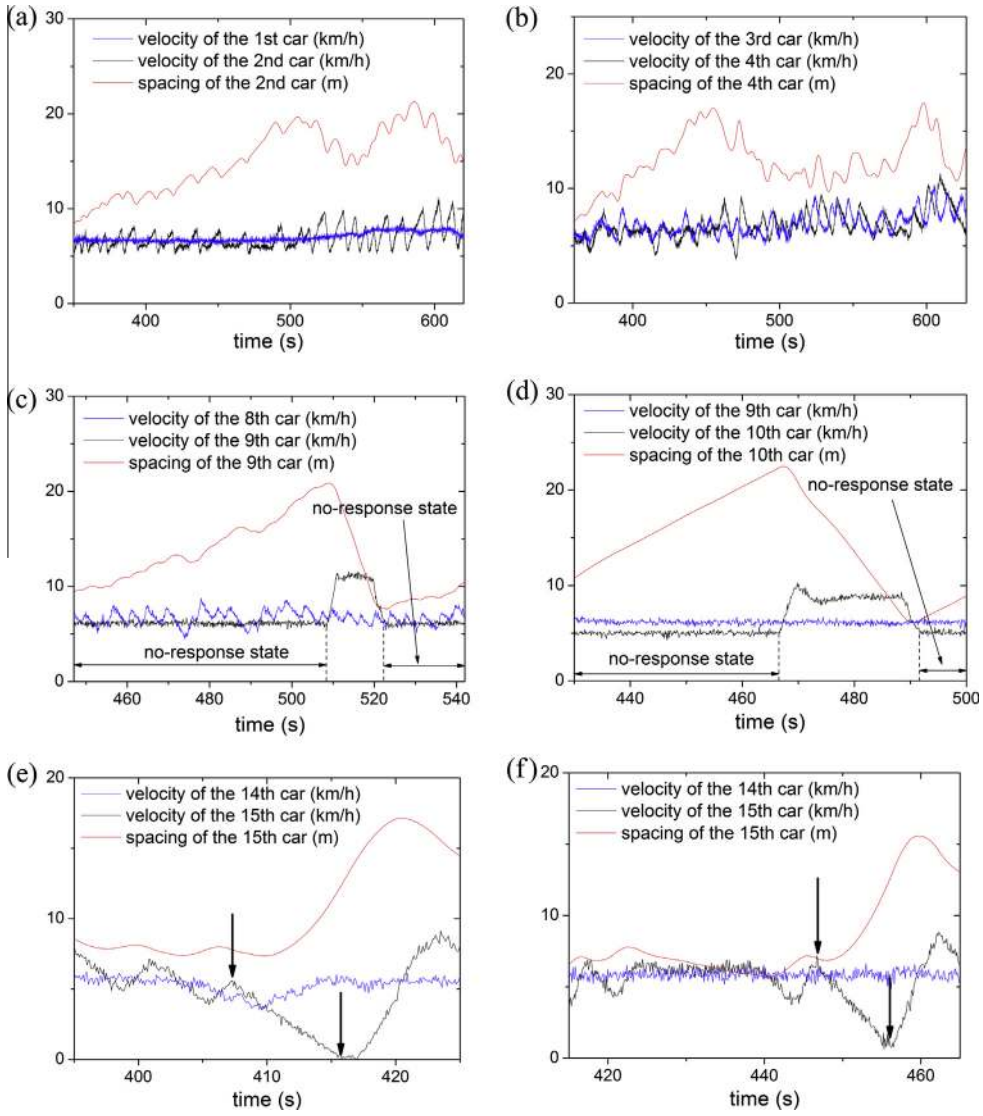

Fig. 8. Several typical examples of the spacing and velocity of the following car as well as the velocity of the preceding car. (a)–(e) is from the run of experiment shown in Fig. 6 and (f) is from the run of experiment shown in Fig. 7.

Fig. 9 shows the simulation results of the velocities of several cars, in which the leading car moves as in the experiment, see Fig. 6(a). The flow rate is about 760 vehicles/h, larger than experimental result, and is very stable. These results show that the IDM fails to reproduce the inhomogeneous state in hypercongestion. This is because cars in the IDM always respond to the change of spacing. As a result, the spacing only slightly fluctuates around the value corresponding to the fundamental diagram. Thus the IDM fails to depict the intrinsic disturbances in hypercongested traffic flow as revealed in Fig. 8.

4.2. Kerner–Klenov model

By using a stochastic three-phase Kerner–Klenov traffic flow model, Kerner (2008) has simulated the structure of hypercongestion. In his simulations, Kerner has studied hypercongested traffic with several different flow rates such as 626, 440, 218, 127 vehicles/h/lane. The simulations show that congested pattern in hypercongestion exhibits non-regular structure, which is consistent with our empirical and experimental data.

4.3. Laval–Leclercq model

Laval and Leclercq (2010) have developed a model, which allows vehicle trajectories to deviate from Newell trajectories. Later Chen et al. (2012a) have generalized the model by considering the timid and aggressive driving behavior. However, in

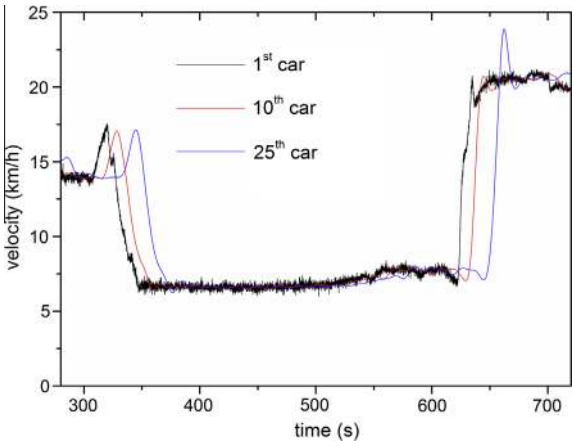

Fig. 9. Simulation results of the velocities of several cars with IDM and specified parameters.

the models, it is assumed that "*vehicle trajectories accord well with Newell' car-following model before they experience traffic oscillations. Namely, a follower's trajectory overlaps its leader's shifted by* (τ, δ)". Here δ can be interpreted as the jam spacing and τ as the wave trip time between two consecutive congested vehicles. This means, if the leading car moves with constant speed, the following car will also move with this constant speed so that their gap remains to be a constant. However, it is not the case in our experiment, as clearly shown in Fig. 8. Therefore, to describe the microscopic traffic behavior accurately, one at least needs to consider stochastic factors, such as in Laval et al. (2014) and Jiang et al. (2014).

4.4. Stochastic Newell model

Laval et al. (2014) has introduced stochastic factors into the deterministic Newell model. In the model, the position and velocity of vehicle n is calculated by

$$x_n(t) = \min[x_n(t-\tau) + \max(\min(\xi_n(t), v_{\max}\tau), 0), x_{n+1}(t-\tau) - \delta]$$

$$v_n(t) = \frac{x_n(t) - x_n(t-\tau)}{\tau}$$

where τ is the wave trip time between two consecutive trajectories and δ is the jam spacing as mentioned before, and $\xi_n(t)$ is the random velocity obtained by generating Normal pseudo-random numbers with the mean and variance determined by

$$E[\xi_n(t)] = v_{\max}\tau - (1 - e^{-\beta\tau})(v_{\max} - v_n(t-\tau))/\beta$$

$$V[\xi_n(t)] = \frac{\sigma^2}{2\beta^3}(e^{-\beta\tau}(4 - e^{-\beta\tau}) + 2\beta\tau - 3)$$

where β is the inverse relaxation time and $\xi_n(t)$ denotes the white noise with diffusion coefficient σ^2.

Now we perform simulations by using the stochastic Newell model to examine whether it can reproduce the inhomogeneous traffic structure in hypercongestion. In the simulation, the following parameter values are adopted: $v_{\max} = 120$ km/h, $\beta = 0.03\ s^{-1}$, $\sigma^2 = 0.49\ m^2\ s^{-3}$, $\delta = 6$ m, and $\tau = 1.2$ s. The simulation results are presented in Fig. 10, which are qualitatively consistent with the experimental ones. This demonstrates that the stochastic factors play an important role in traffic flow dynamics.

4.5. Asymmetric traffic theory

Based on the analysis of the NGSIM trajectory data, Yeo and Skabardonis (2009) proposed an asymmetric traffic theory. The theory assumes that there exists a 2D region enveloped by an acceleration curve and a decelerating curve. Once the traffic state deviates from the 2D region, drivers begin accelerating or decelerating to return to the region. This is very similar to Kerner's three-phase traffic theory. In the 2D region, the coasting state and the stationary state are classified. The stationary phase is defined as near-stationary phase, in which a traffic state remains almost constant with local oscillations due to minor speed adjustment. Coasting is the phase in which the subject vehicle keeps constant speed while its spacing is increased or reduced due to the lead vehicle's acceleration or deceleration. Therefore, in the asymmetric traffic theory, car moves with constant speed in the 2D region. This is different from Kerner's three-phase traffic theory, in which following car adapts its speed to the leading car's speed in the 2D region.

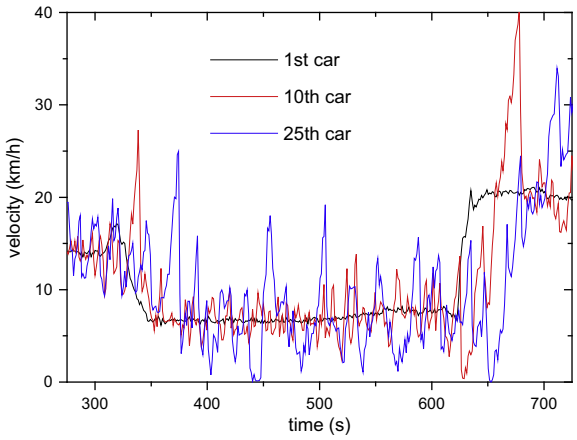

Fig. 10. Simulation results of the velocities of several cars with stochastic Newell model.

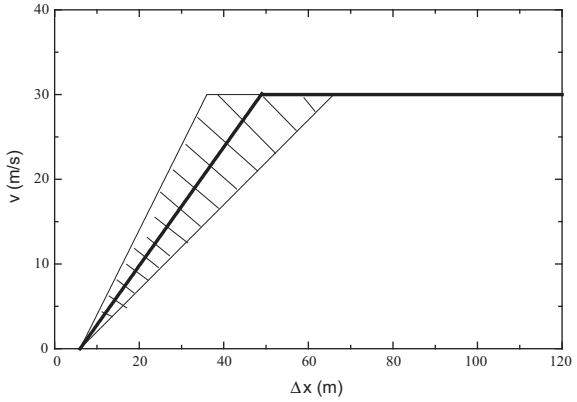

Fig. 11. The two-dimensional region (hatched) and the OV function (thick lines).

To examine the asymmetric traffic theory, we propose a model based on the theory. We suppose in the 2D region, the acceleration of car n

$$dv_n/dt = \varsigma,$$

where ς is a uniformly distributed random number between θ and $-\theta$, which accounts for the stochastic factors. If the state of the car is outside of the region, the car accelerates or decelerates based on the full velocity difference model (Jiang et al., 2001, 2002)

$$\frac{dv_n}{dt} = \kappa[V(\Delta x_n) - v_n] + \lambda \Delta v_n,$$

where V is the optimal velocity (OV) function, κ and λ are sensitivity parameters. $\Delta x_n = x_{n+1} - x_n$ is headway of the car and $\Delta v_n = v_{n+1} - v_n$ is speed difference of the car.

The two-dimensional region is set to be bounded by three straight lines $v = 0.5(\Delta x - 6)$ m/s, $v = (\Delta x - 6)$ m/s, and $v = v_{\max}$. The OV function used is $V(\Delta x) = \max(\min(v_{\max}, 0.7(\Delta x - 6)), 0)$ m/s, see Fig. 11. To avoid car collision, we set $v = 0$ if $\Delta x \leqslant 6$ m. The parameters are set as $\kappa = 0.4\ \mathrm{s}^{-1}$, $\lambda = 0.35\ \mathrm{s}^{-1}$, $v_{\max} = 30$ m/s, $\theta = 0.5$ m/s^2. The simulation results are presented in Fig. 12, which are also able to reproduce the inhomogeneous structure in hypercongestion.

Our test of the models indicates that the formation of inhomogeneous structure in hypercongestion can be qualitatively captured by different models. Therefore, in the future work, quantitative comparisons need to be performed to examine the models and to clarify the underlying generation mechanism of inhomogeneous structure in hypercongestion.

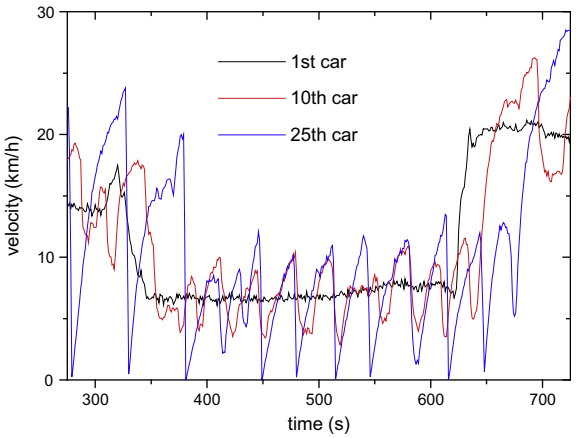

Fig. 12. Simulation results of the velocities of several cars with the model based on asymmetric traffic theory.

5. Conclusion

To understand the spatiotemporal evolution of hypercongestion is not only practically important for congestion mitigation, but also has strong implications on traffic flow modeling. However, due to a lack of precise traffic data, there is a controversy over the structure of hypercongested traffic between traditional two-phase traffic theory and Kerner's three-phase theory.

In this paper, we analyze high resolution, individual vehicle data from both videos and car-following experiments. The traffic states in hypercongested traffic revealed from the microscopic traffic data extracted from the videos on Nanjing airport highway are not homogeneous. Analysis of vehicle trajectories and velocities obtained from an experimental car-following study with a platoon of 25 vehicles also confirms the above findings. The result thus contradicts the existence of a "Homogeneous Congested Traffic" state in hypercongested traffic as claimed in the literature.

Our car-following experiments indicate that in hypercongested traffic, traffic is unstable and small perturbations grow through the platoon over time. We have shown that models such as IDM and Laval–Leclercq model fail to reproduce the phenomenon while models such as stochastic Newell model can. The failure of the IDM and other car-following models to replicate the inhomogeneous states seems to derive from their lack of instability in the density range of hypercongested traffic, and in their one-to-one relation between spacing and speed. These models dictate that drivers respond to even minute changes in spacing, but the empirical evidence shows otherwise. In both the field data and our car-following

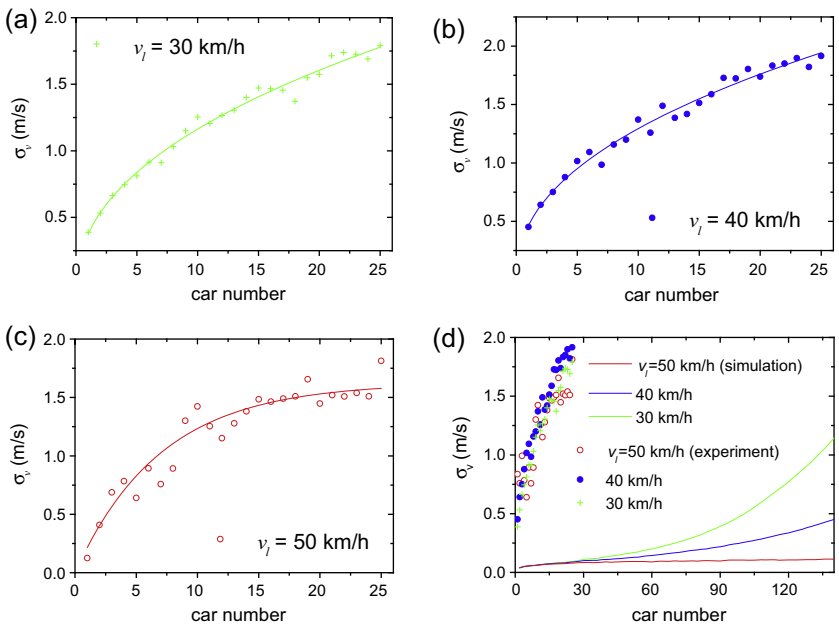

Fig. A1. (a–c) Experimental results of the standard deviation of the velocities along the 25-car-platoon at different leading velocities. The solid line is fitting curve. (d) Comparison between the simulation results of IDM with experimental ones. For details, see Jiang et al. (2014).

experiments, drivers are insensitive to changes in spacing as long as the spacing is within a certain comfort range for a given speed. A remedy is to use a stochastic approach, as were done in Laval et al. (2014) and Kim and Zhang (2008), to model the dynamic relations between spacing and speed.

It is also found from the video traffic data that the structure of hypercongested traffic varies only slightly with location, which might be due to small jams inside hypercongested traffic merging into larger ones slowly and/or larger jams sometimes breaking into small ones. The experimental platoon, unfortunately, is not long enough to permit an examination of how small jams merge into larger ones or how large jams break into small ones. We expect to conduct larger scale experiments in the future to study the condensation of small jams and the breakup of larger jams.

Acknowledgements

We thank the Monitoring Center of Nanjing Airport Highway very much for the support of field data. This work was funded by the National Basic Research Program of China (973 Program No. 2012CB725400), the National Natural Science Foundation of China (Grant Nos. 51338003, 71371175 and 11422221), and the Research Fund for the Doctoral Program of Ministry of Education of China (Grant No. 20123402110060). CJJ acknowledges the support of the Natural Science Foundation of Jiangsu Province (Grant No. BK20150619).

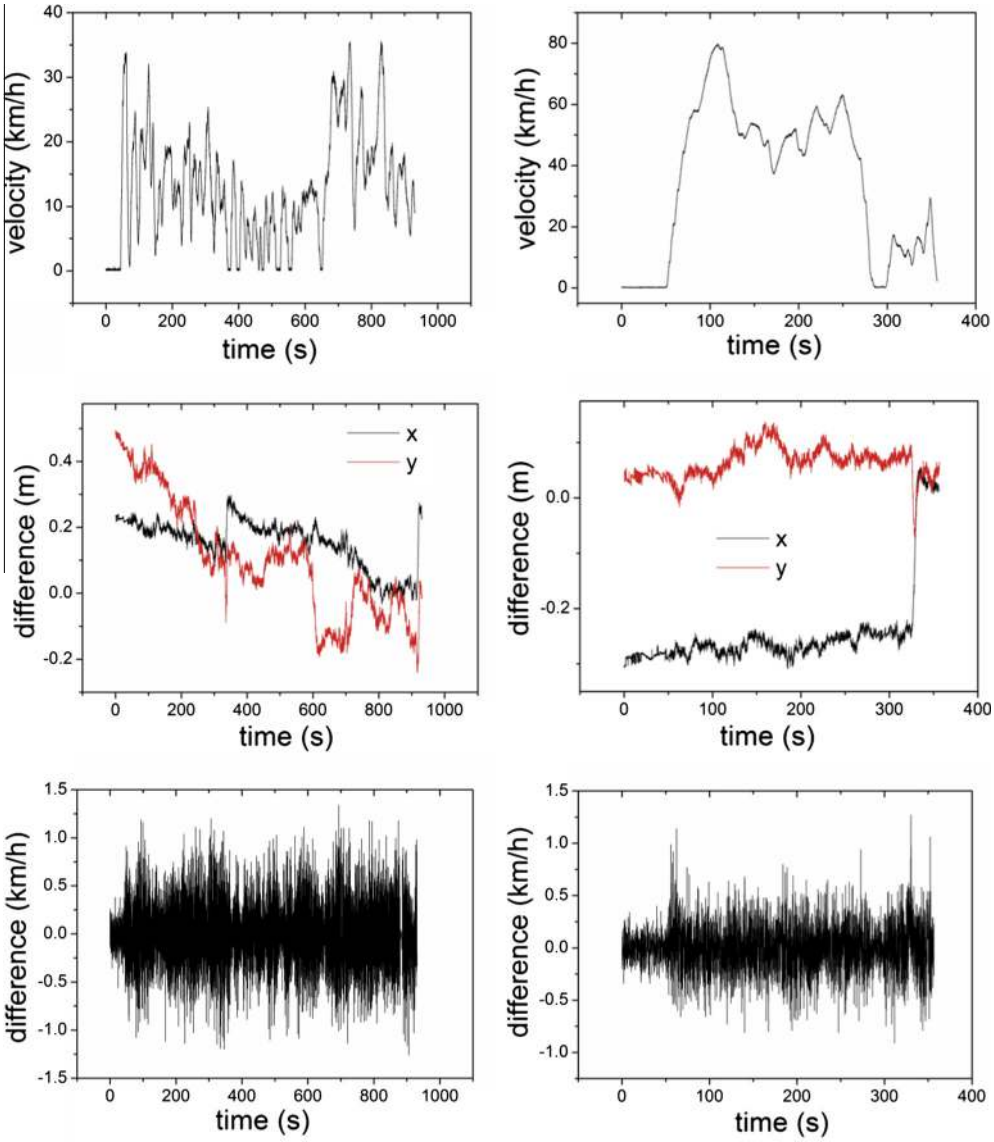

Fig. B1. The measurement differences of the two GPS devices on the 23rd car. The top panels show the velocity of the 23rd car measured by one GPS. The middle panels show the measurement difference of x and y coordination of the two GPS devices. The bottom panels show the measurement difference of velocity of the two GPS devices. The left panels show one example, the right panels show another example.

Appendix A

This appendix shows that the oscillation initially grows in a convex way in the IDM, which are qualitatively different from experimental ones, see figures below (see Fig. A1).

Appendix B

This appendix shows the measure errors of coordination and velocity of two GPS devices on a same car. See the two examples below (see Fig. B1).

We have 27 GPSs, and one failed to work on the experiment day. Therefore, we can install two GPSs in only one car. However, before and after the experiment, we have tested the measurement errors of other GPSs. The errors are within ±1 km/h for speed, and ±1 m for location x and y.

References

Ahn, S., Vadlamani, S., Laval, J.A., 2013. A method to account for non-steady state conditions in measuring traffic hysteresis. Transp. Res. Part C 34, 138–147.
Chen, D., Laval, J.A., Ahn, S., Zheng, Z., 2012a. Microscopic traffic hysteresis in traffic oscillations: a behavioral perspective. Transp. Res. Part B 46, 1440–1453.
Chen, D., Laval, J.A., Zheng, Z., Ahn, S., 2012b. A behavioral car-following model that captures traffic oscillations. Transp. Res. Part B 46, 744–761.
Chen, D., Ahn, S., Laval, J.A., Zheng, Z., 2014. On the periodicity of traffic oscillations and capacity drop: the role of driver characteristics. Transp. Res. Part B 59, 117–136.
Daganzo, C.F., Cassidy, M.J., Bertini, R.L., 1999. Possible explanations of phase transitions in highway traffic. Transp. Res. Part A 33, 365–379.
Farhi, N., 2012. Piecewise linear car-following modeling. Transp. Res. Part C 25, 100–112.
Helbing, D., 2001. Traffic and related self-driven many-particle systems. Rev. Mod. Phys. 73, 1067–1141.
Helbing, D., Hennecke, A., Treiber, M., 1999. Phase diagram of traffic states in the presence of inhomogeneities. Phys. Rev. Lett. 82, 4360–4363.
Jabari, S., Liu, H., 2012. A stochastic model of traffic flow: theoretical foundations. Transp. Res. Part B 46, 156–174.
Jabari, S., Zheng, J., Liu, H., 2014. A probabilistic stationary speed–density relation basedon Newell's simplified car-following model. Transp. Res. Part B 68, 205–223.
Jiang, R., Wu, Q.S., Zhu, Z.J., 2001. Full velocity difference model for a car-following theory. Phys. Rev. E 64, 017101.
Jiang, R., Wu, Q.S., Zhu, Z.J., 2002. A new continuum model for traffic flow and numerical tests. Transp. Res. Part B 36, 405–419.
Jiang, R., Hu, M.B., Zhang, H.M., et al, 2014. Traffic experiment reveals the nature of car-following. PLoS ONE 9 (4), e94351.
Jin, C.J., Wang, W., Jiang, R., Wang, H., 2014. An empirical study of phase transitions from synchronized flow to jams on a single-lane highway. J. Phys. A 47, 125104.
Kerner, B.S., Konhäuser, P., 1993. Cluster effect in initially homogeneous traffic flow. Phys. Rev. E 48, R2335–R2338.
Kerner, B.S., Rehborn, H., 1997. Experimental properties of phase transitions in traffic flow. Phys. Rev. Lett. 79, 4030–4033.
Kerner, B.S., 1998. Experimental features of self-organization in traffic flow. Phys. Rev. Lett. 81, 3797–3800.
Kerner, B.S., 2004. The Physics of Traffic. Springer, Heidelberg.
Kerner, B.S., 2008. A theory of traffic congestion at heavy bottlenecks. J. Phys. A 41, 215101.
Kerner, B.S., 2009. Introduction to Modern Traffic Flow Theory and Control: The Long Road to Three-Phase Traffic Theory. Springer, Berlin.
Kerner, B.S., 2013. Criticism of generally accepted fundamentals and methodologies of traffic and transportation theory: a brief review. Physica A 392, 5261–5282.
Kim, I., Kim, T., Sohn, K., 2013. Identifying driver heterogeneity in car-following based on a random coefficient model. Transp. Res. Part C 36, 35–44.
Kim, T., Zhang, H.M., 2008. A stochastic wave propagation model. Transp. Res. Part B: Methodol. 42, 619–634.
Laval, J.A., Leclercq, L., 2010. A mechanism to describe the formation and propagation of stop-and-go waves in congested freeway traffic. Philos. Trans. R. Soc. A 368, 4519–4541.
Laval, J.A., Toth, C.S., Zhou, Y., 2014. A parsimonious model for the formation of oscillations in car-following models. Transp. Res. Part B 70, 228–238.
Li, L., Chen, X., Li, Z., 2013. Asymmetric stochastic Tau Theory in car-following. Transp. Res. Part F 18, 21–33.
Li, X., Wang, X., Ouyang, Y., 2012. Prediction and field validation of traffic oscillation propagation under nonlinear car-following laws. Transp. Res. Part B 46 (3), 409–423.
Saifuzzaman, M., Zheng, Z., 2014. Incorporating human-factors in car-following models: a review of recent developments and research needs. Transp. Res. Part C 48, 379–403.
Schnetzler, B., Louis, X., 2013. Anisotropic second-order models and associated fundamental diagrams. Transp. Res. Part C 27, 131–139.
Schönhof, M., Helbing, D., 2007. Empirical features of congested traffic states and their implications for traffic modeling. Transp. Sci. 41, 135–166.
Schönhof, M., Helbing, D., 2009. Criticism of three-phase traffic theory. Transp. Res. Part B 43, 784–797.
Treiber, M., Hennecke, A., Helbing, D., 2000. Congested traffic states in empirical observations and microscopic simulations. Phys. Rev. E 62, 1805–1824.
Treiber, M., Kesting, A., Helbing, D., 2010. Three-phase traffic theory and two-phase models with a fundamental diagram in the light of empirical stylized facts. Transp. Res. Part B 44, 983–1000.
Treiber, M., Kesting, A., 2012. Validation of traffic flow models with respect to the spatiotemporal evolution of congested traffic patterns. Transp. Res. Part C 21, 31–41.
Tian, J., Jia, N., Zhu, N., et al, 2014. Brake light cellular automaton model with advanced randomization for traffic breakdown. Transp. Res. Part C 44, 282–298.
Tian, J., Treiber, M., Ma, S., et al, 2015. Microscopic driving theory with oscillatory congested states: model and empirical verification. Transp. Res. Part B 71, 138–157.
Windover, J.R., Cassidy, M.J., 2001. Some observed details of freeway traffic evolution. Transp. Res. Part A 35, 881–894.
Wu, X., Liu, H.X., 2014. Using high-resolution event-based data for traffic modeling and control: an overview. Transp. Res. Part C 42, 28–43.
Yeo, H., Skabardonis, A., 2009. Understanding stop-and-go traffic in view of asymmetric traffic theory. In: 18th International Symposium on Transportation and Traffic Theory, pp. 99–115.
Zheng, Z., Ahn, S., Chen, D., Laval, J.A., 2011a. Applications of wavelet transform for analysis of freeway traffic: bottlenecks, transient traffic, and traffic oscillations. Transp. Res. Part B 45, 372–384.
Zheng, Z., Ahn, S., Chen, D., Laval, J.A., 2011b. Freeway traffic oscillations: microscopic analysis of formations and propagations using wavelet transform. Transp. Res. Part B 45, 1378–1388.

Further reading

Newell, G.F., 2002. A simplified car-following theory: a lower order model. Transp. Res. Part B 36 (3), 195–205.